

Optimization of Copper(I) Thiocyanate as Hole Transport Material for Solar Cell by Scaps-1D Numerical Analysis

Abstract. In SSDSSC, various key parameters of CuSCN as HTM were explored using SCAPS-1D simulation software. A layer thickness of 3 μm with a moderate value of interface defect density was obtained yielding 2.56% of PCE in SSDSSC. TiO_2 ETM and Ni back contact was found to be the best combination with CuSCN HTM in SSDSSC. An excellent temperature gradient in a range between $-0.04\%/K$ and $-0.05\%/K$ was demonstrated, showing that the temperature tolerances of the studied devices are encouraging. In addition, PCE as high as 31.31% has been achieved by substituting the N719 dye with a perovskite absorbent of $\text{CH}_3\text{NH}_3\text{SnI}_3$, and hence exceeding the previously reported PCE value in PSC. Other parameters that have been optimized are retained. Furthermore, the quantum efficiency of such structure has proved that cells with $\text{CH}_3\text{NH}_3\text{SnI}_3$ absorbent layer can absorb a wider range of the light spectrum, enhancing the power conversion efficiency.

Streszczenie. W SSDSSC różne kluczowe parametry CuSCN jako HTM były badane za pomocą oprogramowania symulacyjnego SCAPS-1D. Otrzymano warstwę o grubości 3 μm przy umiarkowanej wartości gęstości defektu powierzchni międzyfazowej, uzyskując 2,56% PCE w SSDSSC. Stwierdzono, że styk tylny TiO_2 ETM i Ni jest najlepszą kombinacją z CuSCN HTM w SSDSSC. Wykazano doskonały gradient temperatury w zakresie od $-0,04\%/K$ do $-0,05\%/K$, co pokazuje, że tolerancje temperaturowe badanych urządzeń są zachęcające. Ponadto PCE tak wysokie jak 31,31% osiągnięto przez zastąpienie barwnika N719 perowskitowym absorbentem $\text{CH}_3\text{NH}_3\text{SnI}_3$, a zatem przekraczając wcześniej podaną wartość PCE w PSC. Pozostałe parametry, które zostały zoptymalizowane, zostają zachowane. Co więcej, wydajność kwantowa takiej struktury dowiodła, że ogniwa z warstwą pochłaniającą $\text{CH}_3\text{NH}_3\text{SnI}_3$ mogą pochłaniać szerszy zakres widma światła, zwiększając efektywność konwersji energii. (Optymalizacja tiocyjanianu miedzi(I) jako materiału transportującego dziury w ogniwach słonecznych za pomocą analizy numerycznej Scaps-1D)

Keywords: CuSCN, Hole Transport Layer, Perovskite Solar Cell, SCAPS-1D, SSDSSC.

Słowa kluczowe: CuSCN, warstwa transportu dziur, Ogniwo słoneczne z perowskitu, SCAPS-1D, SSDSSC.

Introduction

Energy generated from solar cells has been a key element in renewable energy research to fulfil the world energy demand. Theoretically, solar cells convert sunlight into a clean and unlimited form of electrical energy utilizing semiconductor materials. The photovoltaic effect occurs when light or other radiant energy reaches two different contact materials and excites the carriers in the bandgap of the semiconductor [1, 2]. Recently, emerging Solid-State Dye-Sensitized Solar Cell (SSDSSC) and Perovskite Solar Cell (PSC) have remarkably attracted the interest of researchers as an alternative to conventional silicon-based solar cells. The SSDSSC is the extension version of Dye-Sensitized Solar Cells (DSSC) which has been introduced in the early 1990s by O'Regan and Grätzel [1]. Liquid state electrolytes such as organic solvents or ionic liquids in DSSC are replaced by *p*-type inorganic semiconductors, thereby improving the device reliability towards low and high temperatures that haunt the performance of DSSC [3]. In general, the SSDSSC comprises a transparent conducting oxide, a mesoporous metal oxide layer, dye, solid-state Hole-Transporting Materials (HTM) and a metal contact [4, 5].

Copper (I) thiocyanate (CuSCN) is an inorganic *p*-type material in solid-ionized copper molecular form and a promising candidate for use as an HTM layer in SSDSSC [6, 7]. Moreover, CuSCN resources are abundant and relatively inexpensive, consequently further reducing the production costs. In principle, the hole transfer mechanism arises directly from the oxidized dye to the HOMO of the HTM, and thus transports the charges to the counter electrode [8]. In addition, the optical feature allows light absorption to be facilitated over a wide range of wavelengths [9].

The *p*-type CuSCN as an HTM layer in SSDSSC was first introduced by O'Regan *et. al* [10] in 1996. The electrodeposited CuSCN layer shows sufficient transparency characteristics and a decent hole transport mechanism. By annealing, the CuSCN in inert gas or vacuum has further increased the cell efficiency by up to

2% [11]. Recently, numerical studies reported cell efficiency of up to 16.69% was achieved in SSDSSC utilizing CuSCN as the HTM layer and claimed to be among the best materials for HTM [12]. Moreover, the first principal study also revealed that the CuSCN has high optical transparency based on band structure and possess a large bandgap of over 3.5 eV measured by Density Function Theory (DFT) calculations.

Here, the SSDSSC has been successfully simulated using SCAPS-1D software utilizing CuSCN as an HTM layer. The cell efficiency of up to 2.56% was obtained with and without the presence of Ni back contact. However, such efficiencies are obtained from different thicknesses of CuSCN layers which are at 3 μm and 4 μm for with back contact and without back contact, respectively. Nevertheless, the obtained results are less than those reported by previous simulated studies. Past research has ignored the existence of defects at the interface and bulk that would influence the performance of the SSDSSC. Band-tail state may be the cause of the defects that allows the multiple trapping and release phenomena to occur in CuSCN that impede the hole transport mechanism [12].

Methodology - Device simulation

In this work, the SSDSSC and PSC were simulated using the SCAPS software simulator in the 1-dimension structure that has been developed by the Department of Electronics and Information Systems (ELIS) at the University of Gent [14]. Basically, SSDSSC consists of five main components, and here the layers are FTO as front contact, TiO_2 as Electron Transport Material (ETM), N719 as dye-sensitizer, CuSCN as HTM, and Ni as back contact material have been modelled as shown in Fig. 1. Several key parameters concerning the CuSCN layer were analysed to achieve the highest power conversion efficiency (PCE) of SSDSSC. Measurements are set under default illumination of AM1.5G and 100 mW cm^{-2} and 5.24 eV of metal work function for Ni back contact. In this perspective, general SCAPS input parameters for each layer are tabulated in Table 1.

Table 1. The parameters of the SSDSSC's components used in SCAPS-1D simulation

Layer	TiO ₂ [10]	CuSCN [10]	N719 [10]	ZnO [15]	SnO ₂ [16]	CH ₃ NH ₃ SnI ₃ [17]	CH ₃ NH ₃ PbI ₃ [17]
Layer thickness, d (μm)	0.1	Variable	0.05	0.1	0.1	1	1
Bandgap energy, E _g (eV)	3.2	3.6	2.37	3.35	3.6	1.30	1.50
Electron affinity, (eV)	3.9	1.7	3.9	4.5	4	4.20	3.9
Dielectric permittivity, ε (relative)	9	10	30	9	9	10	10
Effective density of conduction band, N _c (cm ⁻³)	1×10 ¹⁹	1×10 ²¹	2.4×10 ²⁰	2.2×10 ¹⁸	2.5×10 ¹⁸	1×10 ¹⁸	2.25×10 ¹⁸
Effective density of valence band, N _v (cm ⁻³)	1×10 ¹⁹	1×10 ²¹	2.5×10 ²⁰	1.8×10 ¹⁹	1.8×10 ¹⁹	1×10 ¹⁸	1×10 ¹⁸
Thermal velocity of electrons, V _e (cm s ⁻¹)	1×10 ⁷	1×10 ⁷	1×10 ⁷	1×10 ⁷	1×10 ⁷	1×10 ⁷	1×10 ⁷
Thermal velocity of holes, V _h (cm s ⁻¹)	1×10 ⁷	1×10 ⁷	1×10 ⁷	1×10 ⁷	1×10 ⁷	1×10 ⁷	1×10 ⁷
Electron mobility, μ _e (cm ² /V _s)	20	100	5	100	100	1.6	2.2
Hole mobility, μ _h (cm ² /V _s)	10	25	5	25	25	1.6	2.2
Density of donors, N _D (cm ⁻³)	1×10 ¹⁶	NA	NA	1×10 ¹⁹	1×10 ¹⁷	NA	NA
Density of acceptors, N _A (cm ⁻³)	NA	Variable	1×10 ¹⁷	NA	NA	3.2×10 ¹⁵	1×10 ¹⁸

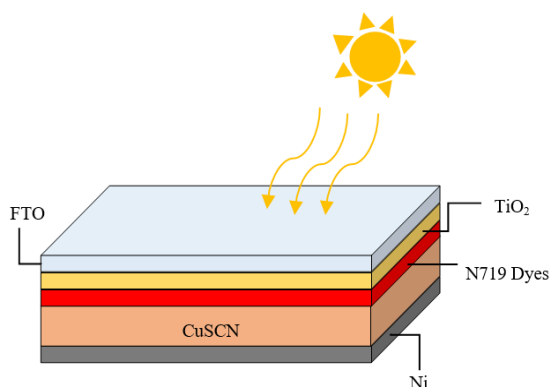


Fig. 1. Solid-state dye-sensitized solar cell structure

Analysis of Different Electron Transport Materials (ETM)

The performance of different ETMs, namely TiO₂, ZnO and SnO₂ were analyzed to obtain the best-employed ETM for SSDSSC application. Among those ETM materials, TiO₂ has demonstrated the best output, achieving up to 2.34% of PCE as illustrated in Fig. 2. Although TiO₂ ETM has shown outstanding results with high efficiency, yet the recombination rate produced is relatively high resulting in poor electron mobility and transport characteristics [18]. This is most probably due to initial oxide layer growth during the anodic process, producing a thicker layer that may consist of dangling bonds or interface defects [19, 20]. The J_{sc} value for TiO₂ was obtained to be 1.5361 mA/cm² which is fairly lower than that found in ZnO and SnO₂ having 1.5372 mA/cm² and 1.5373 mA/cm² respectively, whereas Open-circuit voltage (V_{oc}) did not change much. Inevitably, TiO₂ has shown the optimum PCE of 2.34% compared to ZnO and SnO₂ of 2.20% and 2.18%, respectively. Hence, TiO₂ is a good alternative for the ETM layer.

Analysis of Back Contact Material

A handful of different types of back contact has been simulated as the electrode to the device structure of SSDSSC. The characteristics of each back contact are different, and this affects the efficiency of the solar cell device as shown in Fig. 3. For SSDSSC using Nickel and

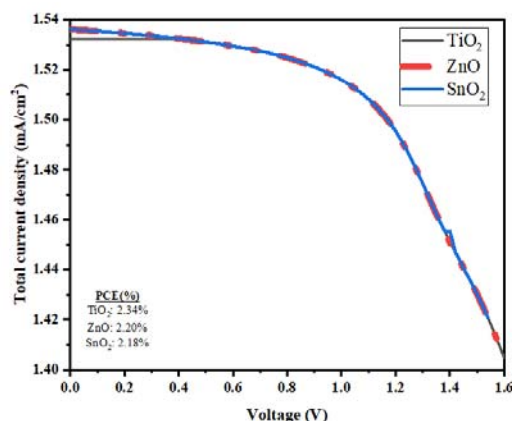


Fig. 2: J-V characteristics of SSDSSC with different types of ETM.

Platinum as back contact has produced a similar cell efficiency of 2.55%, and thus are among the best electrodes to engage. These findings infer that the metal work function plays a strong role, where the high value of the metal work function tends to obtain better efficiency owing to lower barrier height at the metal-semiconductor interface. During applied bias, the band bends and facilitates the flow of electrons, and therefore enhances the ohmic contact characteristics [17,21]. Based on the simulation results obtained, the optimal material for back contact is determined to be Ni, due to its abundant availability and lower cost than Pt, and it is also classified as a non-toxic substance.

Analysis of Variation Thickness CuSCN as HTM

The thickness of the HTM layer plays a key role in achieving the best PCE in SSDSSC. A thinner layer may lead to an incomplete pristine layer that conceals the attribute as a hole carrier. On the other hand, excessive thickness also causes disadvantages to the device performance, notably in terms of the cost of material used as well as the light transparency. Herein, the thickness of CuSCN HTM was varied in the range between 0.1 to 100 μm in SSDSSC. In addition, the presence of back contact was also investigated. It was found that the cell efficiency of

the

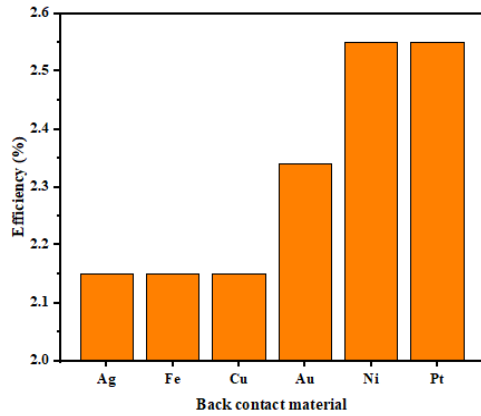


Fig. 2: The cell efficiency of SSDSSC with a variation of back contact materials.

SSDSSC increased with the thickness of the CuSCN HTM layer for both with and without back contact devices. However, the rate of growth began to be slow and became unchanged at layer thicknesses over 3 μm and 4 μm for with back contact and without back contact, respectively as demonstrated in Fig. 4(a), thereby to be the optimum thickness for CuSCN HTM in SSDSSC. At these thicknesses, the PCE of 2.58% and 2.52% were recorded with and without back contact devices of SSDSSC. Initially, as the thickness of the CuSCN HTM layer rises, the absorption of photon would be enhanced and thus provide extra energy to the electrons to be excited into the conduction band and leave holes in the valence band. In that case, more electron-hole pairs will be created in the depletion region [10, 22]. These will gain an excess of carrier concentration and generate higher J_{sc} leading to higher efficiency of SSDSSC.

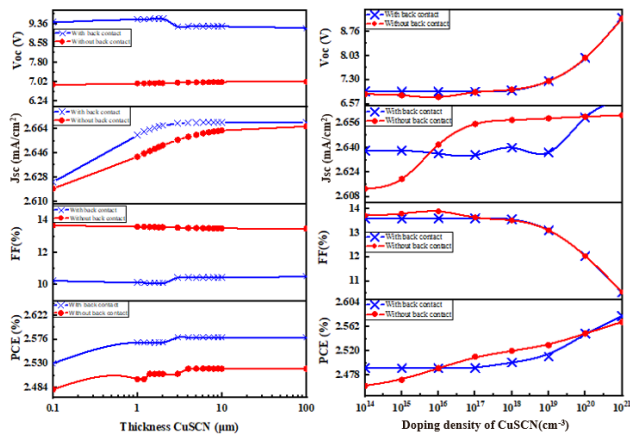


Fig. 4: SSDSSC performance with variable (left) thickness and (right) doping density CuSCN HTM.

Analysis of Working Temperature

Since the ambient temperature between locations varies significantly, therefore the analysis of solar cell performance against temperature becomes important and relevant. In this work, the working temperature was varied at a range between 300 K to 360 K. Fig. 5 shows that the overall cell efficiency in the case of CuSCN HTM in SSDSSC is severely impacted by the working temperature. A downward trend of approximately $-0.04\%/K$ and $-0.05\%/K$ were demonstrated for with and without back contact devices, respectively. With a descending trend of around $-0.4\%/K$ to $-0.5\%/K$ recorded for conventional silicon solar cells, it shows that the CuSCN HTM in SSDSSC is reliable and

excellent towards high temperatures however, its cell efficiency is less than 5% [18, 22]. At higher temperatures, the semiconductor bandgap narrows, causing the crystal lattice to expand and the interatomic bond to weaken [10,23]. This increases thermal energy and attracts additional excited electrons to the conduction band, resulting in a high concentration of intrinsic carriers and rising the saturation current [10, 24].

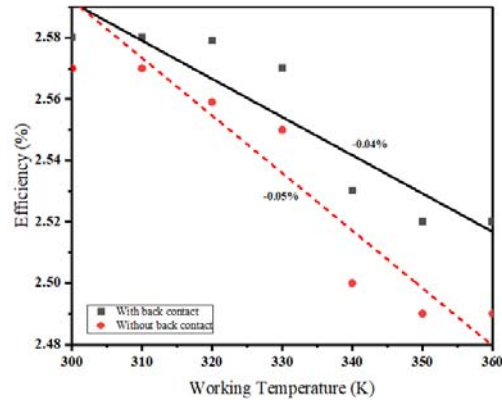


Fig. 5: Temperature dependence of SSDSSC for with and without the presence of Ni back contact devices.

Analysis of Interface Defect

Defect at the interface layer is a widespread dilemma for all semiconductor devices, where it plays a leading role in deteriorating the performance of the semiconductor material. In studying SSDSSC structure, neutral defects at both CuSCN/N719 dye and N719 dye/ TiO_2 interface layers were investigated. At a lower concentration of interface defects, the device performance was not affected, but the cell efficiency started to drop at $1 \times 10^{10} \text{ cm}^{-2}$ and $1 \times 10^{14} \text{ cm}^{-2}$ for CuSCN/N719 dye and N719 dye/ TiO_2 interface layers, respectively as shown in Fig. 6. No significant difference was observed for neither with nor without back contact devices. This indicates that the CuSCN / N719 dye interface is simply impacted by defects, and attention is required during the fabrication process to produce a high-quality interface with fewer defects. Such deficiencies in solar cells allow light to produce heat rather than energy via additional recombination pathways [10,25].

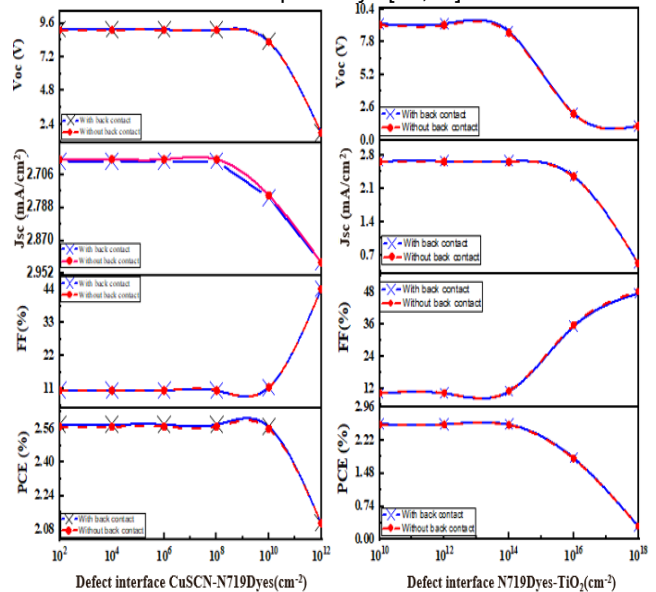


Fig. 6: SSDSSC performance with variation of interface defect density at CuSCN/N719 dye interface (left) and N719 dye/ TiO_2 interface (right)

Furthermore, the high concentration of defect may shorten the carrier diffusion length and thus distort the electron flow [25]. As a result, the interface defect concentration limits were found to be $1 \times 10^{10} \text{ cm}^{-2}$ and $1 \times 10^{14} \text{ cm}^{-2}$ for CuSCN/N719 dye and N719 dye/TiO₂ interface layers, respectively.

Analysis of Efficiency based on Optimum Value for All Parameters with and without Back Contact

The J-V curve for both SSDSSC with and without Ni back contact utilizing the best-optimized parameter in SSDSSC structure is presented in Fig. 7. Given that, both SSDSSCs have achieved a similar optimum cell efficiency of 2.56%, however with a different CuSCN thickness of 3 μm and 4 μm for SSDSSC with and without back contact, respectively. The detailed parameters are shown in Table 2. Based on the outcomes, CuSCN as an HTM layer proves that it is adaptable electrical *p*-type material with great potential to be used in solar cell applications [25]. However, the PCE obtained from the simulated SSDSSC showed unsatisfactory results with merely less than 5%. The capture of light in the N719's dye may have restricted the overall conversion efficiency of this device.

Table 2. The analysis of efficiency based on optimum value for all parameters

Parameter	With back contact	Without back contact
Electron transport material (ETM)	TiO ₂	TiO ₂
Thickness of CuSCN (μm)	3	4
Doping acceptor density of CuSCN, N_A (cm^{-3})	1×10^{21}	
Working temperature (K)	300	
Defect interface (CuSCN/N719) (cm^{-2})	1×10^{10}	
Defect interface (N719/TiO ₂) (cm^{-2})	1×10^{14}	
Open-circuit voltage, V_{OC} (V)	1.2790	1.2787
Short-circuit current density, J_{SC} (mA/cm^2)	2.6577	2.6576
Fill factor (%)	75.31	75.32
PCE (%)	2.56	2.56

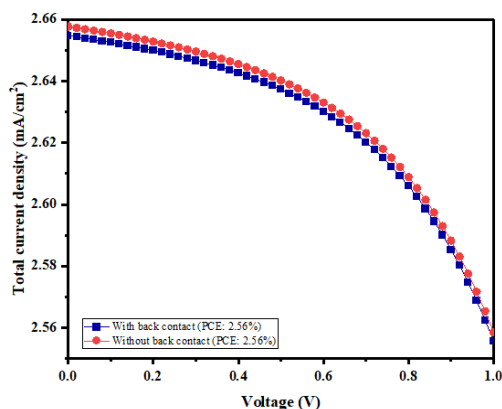


Fig. 7: J-V characteristics for SSDSSC with and without Ni back contact using optimized parameters.

Analysis of Different Absorbent Layer

In this study, the performance of different absorbent layers for SSDSSC with back contact was also investigated by substituting the N719 dye with perovskite layers such as CH₃NH₃PbI₃ and CH₃NH₃SnI₃. All other optimized parameters were retained for this analysis. It is observed that CH₃NH₃SnI₃ has achieved the highest cell efficiency up to 31.31%, compared with CH₃NH₃PbI₃ and N719 dye with 27.90% and 2.56% of PCE, respectively as depicted in Fig.

8. In this sense, CH₃NH₃SnI₃ is a promising absorbent layer, due to its Pb-free characteristics and less expensive. On the other hand, the N719 absorbent layer has produced the lowest cell efficiency, and this can be ascribed to rapid charge recombination, increased electron traffic, or incompatibility between excited energy sources [26].

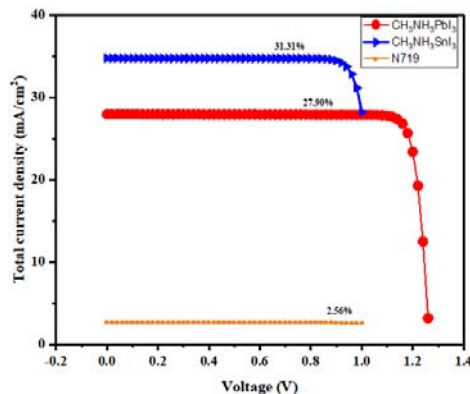


Fig. 8: J-V characteristics of cell using different absorbent layers with the presence of Ni back contact.

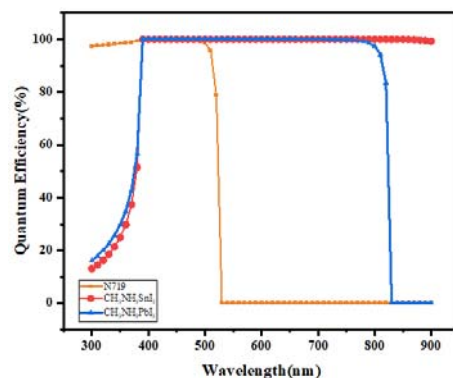


Fig. 9: Quantum efficiency of solar cells using different absorbent layers with the presence of Ni back contact.

Furthermore, the Quantum Efficiency (QE) that can be expressed as a function wavelength or energy analysis was also explored [10,17]. Based on Fig. 9, the CH₃NH₃SnI₃ has shown the best quantum efficiency at almost full percentage in a wide range of wavelengths between 300 nm to 900 nm, thus indicating that sunlight has been actively absorbed by this material. In contrast, CH₃NH₃PbI₃ showed that the absorption wavelength was limited up to 840 nm, whereas the N719 dye absorbs merely one third less than the others absorbent, indicates that the dye suffers in the light absorption process.

Conclusion

In this research, various ETM and back contact materials for possible to be incorporation with CuSCN HTM in SSDSSC have been investigated. TiO₂ ETM and Ni back contact has demonstrated the best cell performance and are hence chosen to be employed in SSDSSC studies. The key parameters of CuSCN HTM have been optimized in generating the highest PCE of SSDSSC. An optimum CuSCN layer thickness of 3 μm with appropriate interface defect density has produced the best PCE of 2.56% in SSDSSC with Ni back contact, yet lower than that in the previously reported study in [11]. Here, the presence of interface defects is considered, and hence the cell performance is reliable and robust. Moreover, replacing N719 with a different absorbent layer of CH₃NH₃SnI₃ has remarkably enhanced the cell efficiency by as high as 31.31%, thus exceeding the previously reported PCE value

in PSC. These findings are supported by QE analysis showing that $\text{CH}_3\text{NH}_3\text{SnI}_3$ can absorb light over a relatively wide range of wavelengths, allowing increased power generation. In addition, a declining trend toward elevated temperature was slightly affected, greater than that found in conventional silicon solar cells. This work thereby provides a clear insight into the possibility of utilizing CuSCN in SSDSSC and particularly in PSC will further increase the power generation, thereby reducing dependence on fossil fuel sources.

Acknowledgement

This work of was supported by Universiti Teknikal Malaysia, Melaka, Malaysia. The work of O. V. Aliyasevram was supported in part by the Zamalah Scheme, Universiti Teknikal Malaysia, Melaka.

REFERENCES

- [1] O'Regan B. and Grätzel M., A low-cost, high-efficiency solar cell based on dye-sensitized colloidal TiO_2 films". *Nature*. 353 (1991) No. 6346, 737–40.
- [2] Crabtree G. W., Lewis N. S., Solar energy conversion, *Phys. Today*, 60 (2007), No. 3, 37–42
- [3] Zhang J., Freitag M., Hagfeldt A., Boschloo G., Solid-State Dye-Sensitized Solar Cells, *Sol. Energy*, (2018), 151-185
- [4] Green M. A., Third generation photovoltaics: Solar cells for 2020 and beyond, *Phys. E Low-Dimensional Syst. Nanostructures*, 14 (2002), No. 1–2, 65–70
- [5] Yan J., Saunders B. R., Third-generation solar cells: A review and comparison of polymer:fullerene, hybrid polymer and perovskite solar cells, *RSC Adv.*, 4 (2014), No. 82, 43286–43314
- [6] Li B., Wang L., Kang B., Wang P., Qiu Y., Review of recent progress in solid-state dye-sensitized solar cells, *Sol. Energy Mater. Sol. Cells*, 90 (2006), No. 5, 549–573
- [7] Nizamuddin A., Arith F., Rong J., Zaimi M., Rahimi A. S., Saat S., Investigation of Copper (I) Thiocyanate (CuSCN) as a Hole Transporting Layer for Perovskite Solar Cells Application, *Journal of Advanced Research in Fluid Mechanics and Thermal Sciences*, (2020) 153-159
- [8] M. Łuszczek, G. Łuszczek, and D. Świsulski, "Simulation investigation of perovskite-based solar cells," *Przegląd Elektrotechniczny*, (2021) 99–102
- [9] Aliyasevram O. V., Arith F., Mustafa A.N., Nor M. K., Al-Ani O., Solution Processed of Solid State HTL of CuSCN Layer at Low Annealing Temperature for Emerging Solar Cell, *International Journal of Renewable Energy Research-IJRER*, (2021) Vol. 11, No. 2
- [10] O'Regan B., Schwartz D. T., Efficient dye-sensitized charge separation in a wide-band-gap p-n heterojunction, *J. Appl. Phys.*, 80 (1996), No. 8, 4749–4754
- [11] Jahantigh F., Safikhani M. J., The effect of HTM on the performance of solid-state dye-sensitized solar cells (SDSSCs): a SCAPS-1D simulation study, *Appl. Phys. A Mater. Sci. Process.*, 125 (2019), No. 4, 1–7
- [12] O'Regan B., Lenzenmann F., Muis R., A solid-state dye-sensitized solar cell fabricated with pressure-treated P25-TiO_2 and CuSCN: Analysis of pore filling and IV characteristics, *Chem. Mater.*, 14 (2002), No. 12, 5023–5029
- [13] Pattanasattayavong, P., Promarak, V., Anthopoulos, T. D., Electronic Properties of Copper(I) Thiocyanate (CuSCN), *Adv. Electron. Mater.* (2017), 3, 1600378.
- [14] Burgelman M., Decock K., Niemegeers A., Verschraegen J., Degraeve S., "SCAPS manual," (2020)
- [15] M. E. A. Aichouba and M. Rahli, Solar cell parameters extraction optimization using Lambert function, *Przegląd Elektrotechniczny*, (2019) Vol. 95
- [16] Shukla V. Panda G., The performance study of CdTe/CdS/SnO₂ solar cell, *Mater. Today Proc.*, 26 (2019), 487–491
- [17] Anwar F., Mahbub R., Satter S. S., Ullah S. M., Effect of Different HTM Layers and Electrical Parameters on ZnO Nanorod-Based Lead-Free Perovskite Solar Cell for High-Efficiency Performance, *Int. J. Photoenergy*, (2017), 1-9
- [18] Yang G., Tao H., Qin P., Ke W., Fang G., Recent progress in electron transport layers for efficient perovskite solar cells, *J. Mater. Chem. A*, 4 (2016), No. 11, 3970–3990
- [19] Meriam Suhaimy S. H., Ghazali N., Arith F., Fauzi B., Enhanced simazine herbicide degradation by optimized fluoride concentrations in TiO_2 nanotubes growth, *Optik*, 212, (2020), No. February, 164651
- [20] Nooraid N. S., Arith F., Alias S. N., Mustafa A. N., Roslan H., Johari S. H., Rahim H. R. A., Ismail M. M., Synthesis of ZnO Nanorod Using Hydrothermal Technique for Dye-Sensitized Solar Cell Application. Intelligent Manufacturing and Mechatronics, *Lecture Notes in Mechanical Engineering. Springer*, (2021)
- [21] Chelvanathan P., Shahahmadi S. A., Arith F., Sobayel K., Aktharuzzaman M., Sopian K., Alharbi F. H., Tabet N., Amin N., Effects of RF magnetron sputtering deposition process parameters on the properties of molybdenum thin films, *Thin Solid Films*, (2017), 638 213–219
- [22] Arith F., Anis S. A. M., Said M. M., Idris C. M. I., Low cost electro-deposition of cuprous oxide P-N homojunction solar cell, *Advanced Materials Research*, 827 (2014), 38–43
- [23] M. S. Tivanov, A. Moskalev, I. A. Kaputskaya, and P. V. Zukowski, "Calculation the ultimate efficiency of pn-junction solar cells taking into account the semiconductor absorption coefficient." *Przegląd Elektrotechniczny*, (2016)
- [24] Azam M. A., Ezyanie N., Aziz A., Fareezuan M., Raja Seman N. A., Suhaili M. R., Abdul Latiff A., Arith F., Mohamed Kassim A., Ani Hanafi M., Structural characterization, and electrochemical performance of nitrogen doped graphene supercapacitor electrode fabricated by hydrothermal method, *International Journal of Nanoelectronics and Materials*, (2021), 127-136
- [25] Wijeyasinghe N., Anthopoulos T. D., Copper (I) thiocyanate (CuSCN) as a hole-transport material for large-area opto / electronics, *Materials*, (2015), 1–45
- [26] Azhari M. A., Arith F., Ali F., Rodzi S., Karim K., Fabrication of low cost sensitized solar cell using natural plant pigment dyes, *ARPN Journal of Engineering and Applied Sciences*, 10 (2015), No. 16, 7092–7096.